

# A Model Prediction-Based Leading Angle Flux Weakening Control Method for Permanent Magnet Synchronous Motor

Xing Zhang<sup>1</sup>, Lin Wang<sup>2</sup>, Yanyan Ye<sup>3</sup>, Lihui Guo<sup>1</sup>, and Yilin Zhu<sup>4,\*</sup>

<sup>1</sup>Xuchang University, Xuchang 461000, China

<sup>2</sup>Beijing Machinery Industry Automation Research Institute Co., Ltd, Beijing 100120, China

<sup>3</sup>State Grid Henan Electric Power Company Xuchang Power Supply Company, Xuchang 461000, China

<sup>4</sup>Jiangsu Changjiang Intelligent Manufacturing Research Institute Co, Ltd, Changzhou 213001, China

**ABSTRACT:** A model prediction based leading angle flux weakening control method is proposed to improve the dynamic and steady-state performance of permanent magnet synchronous motors during the flux weakening process. First, the mathematical model of a permanent magnet synchronous motor is used to construct the prediction model in this method, and then a thorough analysis of the permanent magnet synchronous motor's flux weakening control procedure is carried out. Secondly, based on the principle of model predictive control and the existing delay problems, the corresponding delay compensation method is proposed, and the leading angle flux weakening control method is applied to the proposed model predictive control algorithm, so as to achieve flux weakening speed-up control. Finally, the prototype is used to confirm the effectiveness and precision of the proposed technique. The experimental results show that the leading angle flux weakening control method based on model prediction has faster dynamic response to speed and current than the traditional vector flux weakening control method. At the same time, the steady-state current amplitude is smaller, which has superior current control.

## 1. INTRODUCTION

With the improvement of rare earth material performance and the development of power electronics technology, permanent magnet synchronous motors (PMSMs) gradually surpass traditional induction motors in terms of power factor, operating efficiency, speed stability, torque density, and other performance. Meanwhile, due to the advantages of high power density, high torque density, and wide speed range, PMSMs are widely used as core power units in fields such as aerospace, rail transit, and new energy [1–3]. At present, the model predictive control algorithm is an excellent algorithm for achieving high-performance drive control of the PMSM [4–8]. This method inherits the idea of vector control and achieves closed-loop control by adjusting the  $d$ - and  $q$ -axis current components. However, how to achieve flux weakening speed-up control using model predictive control algorithms is an important research topic.

Many scholars have conducted in-depth research on the flux weakening speed-up algorithm in the process of model predictive control. In [9], the flux weakening control method is combined with model predictive current control to remove the current loop proportional integral (PI) controller and reduce the number of required debugging parameters. In addition, an adaptive flux weakening control method based on voltage feedback is proposed, which can make the parameters of the controller change with speed, thereby improving the dynamic stability performance of the controller. In [10], an equivalent optimization problem is proposed to simplify the complex flux

weakening control problem. However, the matrices  $\mathbf{Q}$  and  $\mathbf{R}$  in this method need to be adjusted appropriately to achieve good weak magnetic control. In [11], a PMSM control method based on explicit model predictive control (MPC) is proposed, which has a new linearization and constraint processing method that can achieve flux weakening control process. In [12], a cost function based model predictive flux control strategy is proposed. This method takes the stator flux vector as the control variable and configures the cost function of the proposed method in the form of flux increment, which can reflect the saturation degree of the inverter output and determine whether to perform flux weakening control by judging the saturation degree. In [13], a flux weakening method based on model predictive direct speed control is proposed. The cost function of this method only includes voltage error, effectively eliminating the influence of weighting factors in traditional model predictive direct speed control methods on control system performance. However, the method is based on whether the motor speed is larger than the turning speed, which can not accurately judge whether the motor is in the flux weakening state, so the efficiency of the motor is affected. In [14], a novel linearization method is adopted to handle the strongly coupled nonlinear interior PMSM mathematical model, and an improved linear object model suitable for constant load torque motors is obtained. By calculating the required  $d$ -axis current, the model predicts flux weakening control. However, the basis for determining whether to enter a flux weakening state using this method is also the turning speed value, so it will also have an impact on the efficiency of the motor.

\* Corresponding author: Yilin Zhu (yl.zhu.dy@gmail.com).

The aforementioned techniques have been used to study flux weakening speed-up algorithms for various kinds of model predictive control. Nevertheless, little research on flux weakening speed-up has been conducted for the finite set model predictive control technique presented in this paper. In view of this, this article proposes a model prediction-based leading angle flux weakening control (MP-LAFWC) algorithm based on the model predictive current control algorithm. This algorithm adopts the conventional  $i_d = 0$  control method before the motor enters the flux weakening control process, and the  $q$ -axis current is adjusted through the model prediction algorithm. When the motor enters a flux weakening state, the  $d$ -axis current is calculated through the leading angle, and the calculated  $d$ -axis and  $q$ -axis currents are fed into the MPC algorithm for adjustment, and closed-loop control is completed. Therefore, this algorithm can not only achieve operation below the turning speed, but also achieve flux weakening operation above the turning speed.

## 2. MATHEMATICAL MODEL AND FLUX WEAKENING CONTROL ANALYSIS

### 2.1. Model Predictive Control Mathematical Model

In the process of vector control, the stator voltage equation in the rotating coordinate system is more applicable, and the expression in the  $d$ - and  $q$ -axis rotating coordinate system is:

$$\begin{bmatrix} u_d \\ u_q \end{bmatrix} = \begin{bmatrix} R + pL_d & -\omega_e L_q \\ \omega_e L_d & R + pL_q \end{bmatrix} \begin{bmatrix} i_d \\ i_q \end{bmatrix} + \begin{bmatrix} 0 \\ \omega_e \lambda_f \end{bmatrix} \quad (1)$$

where the subscripts  $d$  and  $q$  respectively represent the coordinate axes corresponding to the rotating coordinate system. Therefore,  $i_d$ ,  $i_q$ ,  $L_d$ ,  $L_q$ ,  $u_d$ , and  $u_q$  are the current, inductance, and voltage components corresponding to the coordinate axis.  $R$  represents stator resistance,  $\lambda_f$  the flux linkage of permanent magnet,  $\omega_e$  the rotor angular velocity value. In surface mounted permanent magnet synchronous motors (SPMSMs), there exists  $L_d = L_q = L_s$  because the  $d$ - and  $q$ -axis reluctances are equal.

When the motor operates stably at high speed, the back electromotive force will reach the maximum value that the inverter can output, which is much greater than the voltage drop value generated by the resistance. Therefore, the stator resistance part and current differential term in (1) can be ignored. (1) can be simplified as:

$$\begin{bmatrix} u_d \\ u_q \end{bmatrix} = \begin{bmatrix} 0 & -\omega_e L_q \\ \omega_e L_d & 0 \end{bmatrix} \begin{bmatrix} i_d \\ i_q \end{bmatrix} + \begin{bmatrix} 0 \\ \omega_e \lambda_f \end{bmatrix} \quad (2)$$

Formula (1) can be transformed into current form since the motor control mechanism mostly takes the form of current. Formula (1) is discretized using the forward Euler method in the meantime to make it easier to understand the states of the current at different times, with the specific form shown below.

$$\begin{bmatrix} i_d(k+1) \\ i_q(k+1) \end{bmatrix} = \begin{bmatrix} \left(1 - \frac{R}{L_s} T_s\right) & \omega_e(k) T_s \\ -\omega_e(k) T_s & \left(1 - \frac{R}{L_s} T_s\right) \end{bmatrix} \begin{bmatrix} i_d(k) \\ i_q(k) \end{bmatrix}$$

$$+ \frac{T_s}{L_s} \begin{bmatrix} u_d(k) \\ u_q(k) \end{bmatrix} - \begin{bmatrix} 0 \\ \frac{\omega_e(k) \lambda_f}{L_s} T_s \end{bmatrix} \quad (3)$$

where  $(k)$  and  $(k+1)$  represent the corresponding states of the parameters at the current time and the next time, respectively, while  $T_s$  represents the control period.

### 2.2. Model and Analysis of Flux Weakening Control

The value of the back electromotive force is also steadily increasing as the PMSM accelerates. If alternative control strategies are not applied, the inverter's maximum voltage output will prevent the motor speed from rising further. The back electromotive force's magnitude is determined by the product of the motor's electric angular velocity and the permanent magnet's magnetic flux. While the back electromotive force value approaches the maximum value of the power supply, the motor speed cannot continue to increase using the original control algorithm since the permanent magnet flux in the motor is constant. The speed needs to be increased further, hence a flux weakening control mechanism must be implemented [15–18].

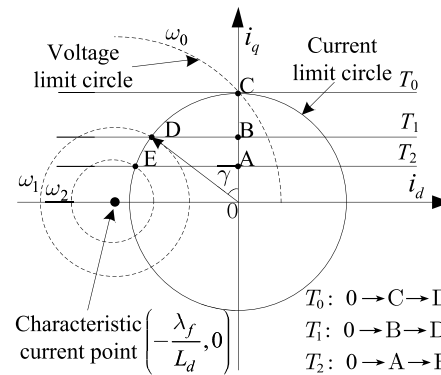


FIGURE 1. The trajectory of the current operating state.

The angle between the stator current  $i_s$  and the  $q$ -axis will continue to grow as a result of the negative directionally increasing  $d$ -axis current during this operation. The current leading angle, shown as  $\gamma$  in Fig. 1, is defined as the angle between  $i_s$  and the  $q$ -axis in the aforementioned setting. When the current leading angle  $\gamma = 0$ , it is a conventional  $i_d = 0$  control. The larger the current leading angle  $\gamma$  is, the deeper the degree of weakening magnetic field is. The stator voltage of the motor is limited by the capacity of the inverter, and the voltage vector during stable operation satisfies (4).

$$u_s^2 = u_d^2 + u_q^2 \leq U_{\max}^2 \quad (4)$$

where  $u_s$  is the stator voltage.

After substituting (2) into (4), it can be obtained that:

$$(L_q i_q)^2 + (L_d i_d + \lambda_f)^2 \leq \frac{U_{\max}^2}{\omega_e^2} \quad (5)$$

The stator current  $i_s$  is limited by the power device's capability, and the output value is similarly constrained. The maximum value of the current  $I_{\max}$  conforms to the following form:

$$i_s^2 = i_d^2 + i_q^2 \leq I_{\max}^2 \quad (6)$$

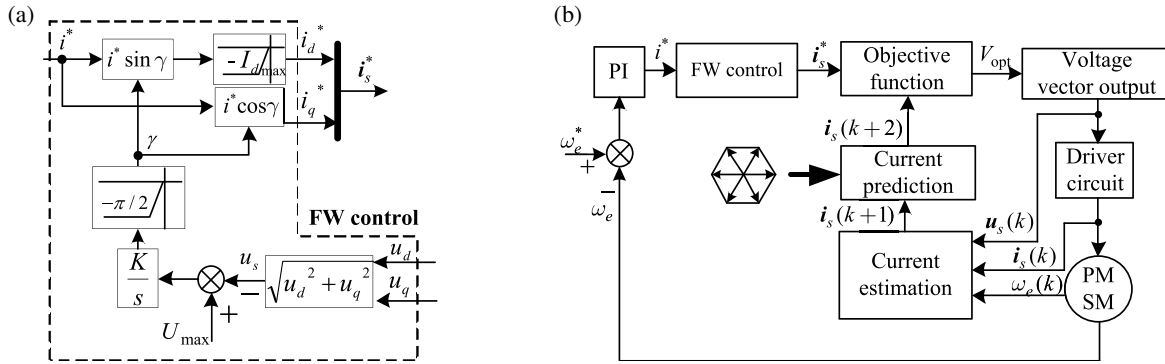


**FIGURE 2.** The control block diagram of the MP-LAFWC. (a) Leading angle flux weakening control block diagram. (b) Total block diagram.

According to (5), voltage related constraints can be plotted as shown in Fig. 1, and the trajectory equation satisfies the form of an elliptical equation. When the inductance coefficients of the  $d$ - and  $q$ -axes are equal, the elliptical curve will become a circle. Meanwhile, according to (6), the circular trajectory at maximum current can be plotted.

In Fig. 1, where the characteristic current point's theoretical calculation value ( $i_d = -\lambda_f/L_d$ ) is outside the current limit circle, and the trajectory of the current operating state is plotted using the data from the experimental prototype parameters. We shall conduct analysis using this example.

The motor's rotational speed, when the stator voltage approaches the maximum the inverter can produce, is known as the turning speed. The field oriented control approach of  $i_d = 0$  is typically employed when the speed of the SPMSM is slower than the turning speed. To produce torque, all of the stator current  $i_s$  in this approach is situated on the  $q$ -axis. It is clear from Fig. 1 that the leading angle  $\gamma = 0$  at this moment. If the load torque is  $T_1$ , the current should be at point B. The power supply will then no longer be able to deliver the higher level voltage value needed for speed expansion because the back electromotive force generated by the SPMSM will reach the limit value of the inverter output when the speed exceeds the turning speed. Only by reducing the magnetic field of the permanent magnet can the speed be increased at this moment. The specific implementation process is to gradually increase the current in the  $d$ -axis direction, which reduces the amplitude of the air gap magnetic flux. From the analysis in Fig. 1, it is found that the leading angle  $\gamma$  gradually increases; the speed reaches  $\omega_1$ ; the operating state of the current is  $B \rightarrow D$ . In a similar manner, if the load torque is  $T_2$  ( $T_1 > T_2$ ), the speed stabilizes to  $\omega_2$ , the trajectory of the entire current is  $O \rightarrow A \rightarrow E$ . If the torque is  $T_0$  ( $T_0 > T_1 > T_2$ ), the speed needs to increase to  $\omega_1$ , and the trajectory of the entire current is  $O \rightarrow C \rightarrow D$  [19].

At the same time, we also find that during the flux weakening control process, the  $d$ -axis component  $i_d$  is increasing negatively, and the  $q$ -axis current component  $i_q$  is decreasing. According to the motor torque expression, the flux weakening process is bound to lose part of the torque performance, which is also a compromise between speed and torque.

### 3. MODEL PREDICTIVE FLUX WEAKENING CONTROL METHOD

#### 3.1. Analysis of Model Predictive Control Principle and Delay Compensation

The basic principle of finite set model predictive control is to control the motor using the inverter's constrained set of voltage vectors. First, establish a corresponding prediction model based on the PMSM mathematical model, and then use the voltage and current that have been sampled to determine the next predicted current. The next drive control process is then completed by applying the corresponding switch state of the variable to the inverter drive after the optimal control variable has been chosen using the defined cost function [20].

In actual control systems, system delay is inevitable due to the influence of hardware and digital control systems. It means that the optimal voltage vector selected using the cost function in the current control cycle needs to be applied to the motor at the next moment, which will lead to poor performance of the entire control system. Therefore, it is necessary to perform one shot delay compensation on the system.

The currents at  $(k+2)$  can be expressed as follows because  $(k+2)$  stands for the time corresponding to delay compensation:

$$\begin{bmatrix} i_d(k+2) \\ i_q(k+2) \end{bmatrix} = \begin{bmatrix} \left(1 - \frac{R}{L_s} T_s\right) & \omega_e(k) T_s \\ -\omega_e(k) T_s & \left(1 - \frac{R}{L_s} T_s\right) \end{bmatrix} \begin{bmatrix} i_d(k+1) \\ i_q(k+1) \end{bmatrix} + \frac{T_s}{L_s} \begin{bmatrix} u_d(k+1) \\ u_q(k+1) \end{bmatrix} - \begin{bmatrix} 0 \\ \frac{\omega_e(k) \lambda_f T_s}{L_s} \end{bmatrix} \quad (7)$$

where  $(k+1)$  and  $(k+2)$  represent the predicted values at the moment of  $(k+1)$  and  $(k+2)$ , respectively. Since the mechanical variable changes at a much smaller rate than the electrical variable, the rotational speed is considered constant for the unit control cycle.

The  $d$ - and  $q$ -axis voltages at time  $(k+1)$  in (7) can be calculated using the following formula:

$$\begin{bmatrix} u_d(k+1) \\ u_q(k+1) \end{bmatrix} = \begin{bmatrix} \cos \theta_e(k) & \sin \theta_e(k) \\ -\sin \theta_e(k) & \cos \theta_e(k) \end{bmatrix} \begin{bmatrix} u_\alpha(k) \\ u_\beta(k) \end{bmatrix} \quad (8)$$

Parameters	Value
Stator resistance $R$ ( $\Omega$ )	1.6
Inductance $L_s$ (H)	0.005075
Pole Pairs	4
Permanent magnet flux $\lambda_f$ (Wb)	0.0825
Rated speed $n_N$ (r/min)	3000
Rated power $P$ (kW)	0.2
Rated voltage $U$ (V)	220
Rated current $I$ (A)	2.1
Rated torque $T_e$ (N·m)	0.64

TABLE 1. Parameters of the prototype.

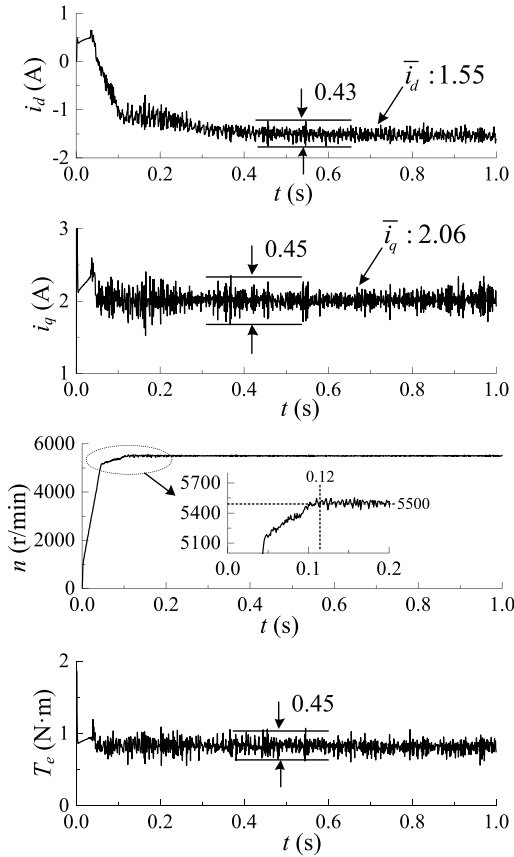


FIGURE 4. Waveforms of the traditional vector flux weakening control.

where  $u_\alpha$  and  $u_\beta$  are obtained by voltage reconstruction, respectively, where  $u_\alpha$  and  $u_\beta$  can be reconstructed from the DC bus voltage value and the driving signal.

The two-level three-phase voltage source inverter can generate 8 basic voltage vectors, including 6 non-zero voltage vectors and 2 zero vectors. After the delay compensation, the predicted current becomes the form shown in (7), and the compensated predicted current is brought into the cost function shown in (9) for calculation and performance evaluation, and the switching state with the smallest cost function value is calculated. Finally, the obtained switching state is applied to the drive control of the power device to realize the model predictive control. Here, the cost function is calculated using the following form.

$$J = [i_d^* - i_d(k+2)]^2 + [i_q^* - i_q(k+2)]^2 \quad (9)$$

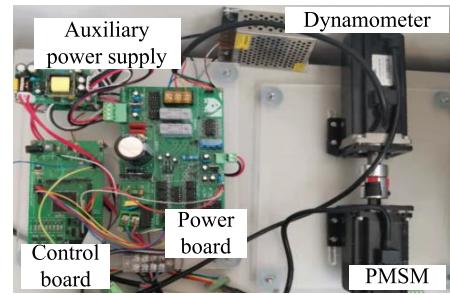


FIGURE 3. Schematic diagram of the experimental platform.

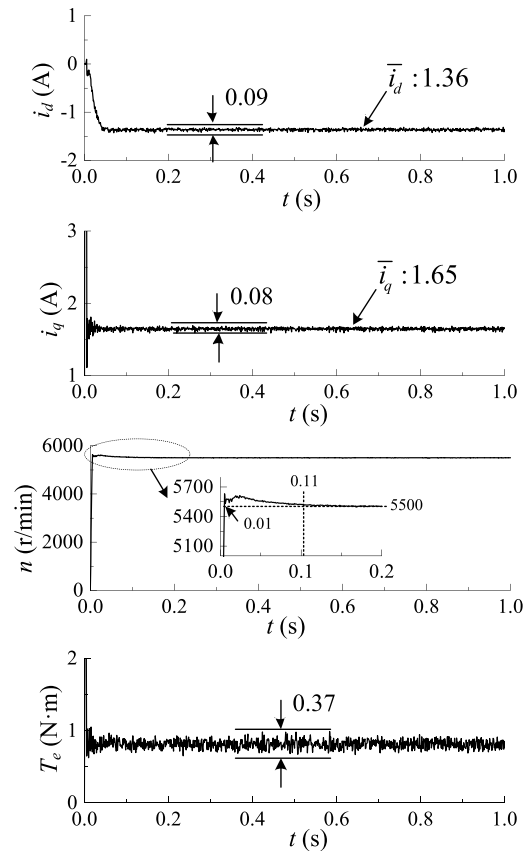


FIGURE 5. Waveforms of the MP-LAFWC.

### 3.2. The Proposed Model Prediction-Based Leading Angle Flux Weakening Control Method

The control block diagram of the MP-LAFWC method proposed in this article is shown in Fig. 2, where the leading angle flux weakening control algorithm is shown in Fig. 2(a). Through the formula shown in (4) to calculate the stator voltage and with the voltage limit value  $U_{max}$  for difference, integration, and limiting operations, the required leading angle  $\gamma$  can be finally obtained, according to the leading angle shown in Fig. 1, and the stator current  $i^*$  projected on the  $d$ - and  $q$ -axes can be used as a reference value for the  $d$ - and  $q$ -axis currents. When the stator voltage  $u_s$  is less than or equal to the voltage limit value  $U_{max}$ , the output result of the leading angle  $\gamma$  is 0, then  $i_d^* = 0$ . When the stator voltage  $u_s$  is greater than the volt-

age limit value  $U_{\max}$ , the output result of the leading angle  $\gamma$  is negative and is limited within  $-\pi/2$ . At this time, the current distribution process is consistent with the current change process analyzed in Fig. 1.

After the design of the flux weakening control algorithm is completed, it is applied to the MPC algorithm block diagram shown in Fig. 2(b). By calculating the allocated stator current  $\bar{i}_s^*$  and the predicted current  $\bar{i}_s(k+2)$ , the optimized voltage  $V_{\text{opt}}$  is obtained. The motor is driven and controlled through voltage vector output and driving circuit.

#### 4. EXPERIMENT AND ANALYSIS

In order to verify the control performance of the proposed method, an experimental platform as shown in Fig. 3 is built, and experiments based on MP-LAFWC are conducted on this platform. In the experimental platform, the main control unit selected is TI's TMS320F28335, and the power drive module uses Mitsubishi's intelligent power module PS21965. The basic parameters of the testing motor are shown in Table 1. Due to the mechanical structure limitations of the encoder, the experimental speed tested is 5500 r/min, and the load torque is rated at 0.64 N·m. The proposed method is compared with traditional vector flux weakening control method. Among them, the parameters of the speed loop PI controller are  $k_p = 0.01$  and  $k_i = 0.002$ . The integral coefficient in leading angle flux weakening control is 0.0002.

Figure 4 shows the waveform of  $d$ - and  $q$ -axis currents, speed, and torque under traditional vector flux weakening control. From these figures, it can be seen that the average  $d$ -axis current of the motor at steady state after entering a flux weakening state is  $\bar{i}_d = 1.55$  A, with a fluctuation range of 0.43 A. Average  $q$ -axis current at steady state  $\bar{i}_q = 2.06$  A, with a fluctuation range of 0.45 A. In the speed waveform, the given speed of 5500 r/min is reached for the first time at 0.12 s. The fluctuation amplitude of the torque waveform in steady-state is 0.45 N·m.

Figure 5 shows the waveform of  $d$ - and  $q$ -axis currents, speed, and torque for the proposed method. From these figures, it can be seen that the average  $d$ -axis current of the motor at steady state after entering a flux weakening state is  $\bar{i}_d = 1.36$  A, and the fluctuation amplitude is 0.09 A. Compared with traditional vector flux weakening control method, the average  $d$ -axis current  $\bar{i}_d$  is decreased by 12.26% and the fluctuation amplitude decreased by 79.07%. Average  $q$ -axis current at steady state  $\bar{i}_q = 1.65$  A, and the fluctuation amplitude is 0.08 A. Compared with traditional vector flux weakening control method, the average  $q$ -axis current  $\bar{i}_q$  is decreased by 19.90% and the fluctuation amplitude decreased by 82.22%. In the speed waveform, the given speed of 5500 r/min is first reached at 0.01 s, and then the given speed is reached again at 0.11 s and remained stable thereafter. The fluctuation amplitude of the torque waveform in steady-state is 0.37 N·m, which is reduced by 17.78% compared to the traditional vector flux weakening control method.

#### 5. CONCLUSION

High performance and efficient flux weakening control has always been a hot topic in the motor control process. This paper

proposes a model prediction-based leading angle flux weakening control algorithm. This method can adjust the current through model predictive control algorithm after the motor enters the flux weakening state, achieving fast speed control. The experimental results show that the proposed method has faster speed and current dynamic response than traditional vector flux weakening control method. At the same time, the steady-state current amplitude is smaller, and it has better current control performance.

#### REFERENCES

- [1] Liu, X., Y. Pan, Y. Zhu, H. Han, and L. Ji, "Decoupling control of permanent magnet synchronous motor based on parameter identification of fuzzy least square method," *Progress In Electromagnetics Research M*, Vol. 103, 49–60, 2021.
- [2] Zhu, L., B. Xu, and H. Zhu, "Interior permanent magnet synchronous motor dead-time compensation combined with extended Kalman and neural network bandpass filter," *Progress In Electromagnetics Research M*, Vol. 98, 193–203, 2020.
- [3] Gao, M., H. Zhu, and Y. Shi, "Predictive direct control of permanent magnet assisted bearingless synchronous reluctance motor based on super twisting sliding mode," *Progress In Electromagnetics Research M*, 2021.
- [4] Li, X., W. Tian, X. Gao, Q. Yang, and R. Kennel, "A generalized observer-based robust predictive current control strategy for pmsm drive system," *IEEE Transactions on Industrial Electronics*, Vol. 69, No. 2, 1322–1332, Feb. 2022.
- [5] Niu, S., Y. Luo, W. Fu, and X. Zhang, "Robust model predictive control for a three-phase pmsm motor with improved control precision," *IEEE Transactions on Industrial Electronics*, Vol. 68, No. 1, 838–849, Jan. 2021.
- [6] Wang, Z., A. Yu, X. Li, G. Zhang, and C. Xia, "A novel current predictive control based on fuzzy algorithm for PMSM," *IEEE Journal of Emerging and Selected Topics in Power Electronics*, Vol. 7, No. 2, 990–1001, Jun. 2019.
- [7] Zhang, X., L. Zhang, and Y. Zhang, "Model predictive current control for PMSM drives with parameter robustness improvement," *IEEE Transactions on Power Electronics*, Vol. 34, No. 2, 1645–1657, Feb. 2019.
- [8] Zhang, Y., J. Jin, and L. Huang, "Model-free predictive current control of PMSM drives based on extended state observer using ultralocal model," *IEEE Transactions on Industrial Electronics*, Vol. 68, No. 2, 993–1003, Feb. 2021.
- [9] Zhang, Y., J. Jin, H. Jiang, and D. Jiang, "Adaptive PI parameter of flux-weakening controller based on voltage feedback for model predictive control of SPMSM," in *2020 IEEE Energy Conversion Congress and Exposition (ECCE)*, 2674–2681, IEEE, Detroit, MI, USA, Oct. 10-15, 2020.
- [10] Zhang, Y. and R. Qi, "Flux-weakening drive for IPMSM based on model predictive control," *Energies*, Vol. 15, No. 7, Apr. 2022.
- [11] Mynar, Z., L. Vesely, and P. Vaclavek, "PMSM model predictive control with field-weakening implementation," *IEEE Transactions on Industrial Electronics*, Vol. 63, No. 8, 5156–5166, Aug. 2016.
- [12] Zheng, Z. and D. Sun, "Model predictive flux control with cost function-based field weakening strategy for permanent magnet synchronous motor," *IEEE Transactions on Power Electronics*, Vol. 35, No. 2, 2151–2159, Feb. 2020.
- [13] Zhang, X., Z. Zhao, and C. Xu, "A flux-weakening method for PMSM based model predictive direct speed control," in *2020*

- IEEE 9th International Power Electronics and Motion Control Conference (IPEMC2020-ECCE Asia)*, 2557–2561, IEEE, Nanjing, China, Nov. 29–Dec. 2, 2020.
- [14] Liu, J., C. Gong, Z. Han, and H. Yu, “IPMSM model predictive control in flux-weakening operation using an improved algorithm,” *IEEE Transactions on Industrial Electronics*, Vol. 65, No. 12, 9378–9387, Dec. 2018.
- [15] Zhou, K., M. Ai, D. Sun, N. Jin, and X. Wu, “Field weakening operation control strategies of PMSM based on feedback linearization,” *Energies*, Vol. 12, No. 23, Dec. 2019.
- [16] Ding, D., G. Wang, N. Zhao, G. Zhang, and D. Xu, “Enhanced flux-weakening control method for reduced DC-link capacitance IPMSM drives,” *IEEE Transactions on Power Electronics*, Vol. 34, No. 8, 7788–7799, Aug. 2019.
- [17] Deng, T., Z. Su, J. Li, P. Tang, X. Chen, and P. Liu, “Advanced angle field weakening control strategy of permanent magnet synchronous motor,” *IEEE Transactions on Vehicular Technology*, Vol. 68, No. 4, 3424–3435, Apr. 2019.
- [18] Miguel-Espinar, C., D. Heredero-Peris, G. Gross, M. Llonch-Masachs, and D. Montesinos-Miracle, “Maximum torque per voltage flux-weakening strategy with speed limiter for PMSM drives,” *IEEE Transactions on Industrial Electronics*, Vol. 68, No. 10, 9254–9264, Oct. 2021.
- [19] Pan, Y., X. Liu, Y. Zhu, and L. Z., “A leading angle flux weakening control method for PMSM based on active disturbance rejection control,” *Progress In Electromagnetics Research C*, Vol. 121, 29–38, 2022.
- [20] Liu, X., Y. Pan, L. Wang, J. Xu, Y. Zhu, and Z. Li, “Model predictive control of permanent magnet synchronous motor based on parameter identification and dead time compensation,” *Progress In Electromagnetics Research C*, Vol. 120, 253–263, 2022.